2008-01-01

Investigation on Singlemode-multimode-singlemode Fiber Structure

Qian Wang

Gerald Farrell
Technological University Dublin, gerald.farrell@tudublin.ie

W. Yan

Recommended Citation

Wang, Q., Farrell, G., Yan, W.: Investigation on singlemode-multimode-singlemode fiber structure. *IEEE Journal of Lightwave Technology*, 2008, Vol.26, no. 5, pp.512-519. doi:10.1109/JLT.2007.915205

Investigation on Single-Mode–Multimode–Single-Mode Fiber Structure

Qian Wang, Gerald Farrell, and Wei Yan

***Abstract*—This paper presents an investigation on a single-mode–multimode–single-mode fiber structure. A one-way guided-mode propagation analysis for the circular symmetry waveguide is employed to model the light propagation and the approximated formulations are derived and evaluated concerning the accuracy. Phase conjunction of the multimode interference within the fiber structure is revealed. A simple way to predict and analyze the spectral response of the structure is presented through the space to wavelength mapping with the derived approximated formulations. The prediction of spectral response is verified numerically and experimentally.**

***Index Terms*—Fiber optics, multimode interference.**

I. Introduction

THE multimode interference (MMI) in a planar waveguide has been intensively investigated and the self-imaging of the input light field is well known and widely employed in developing beam splitters, combiners and multiplexers for optical communications [1]–[3]. Recently, the multimode interference occurring in a single-mode–multimode–single-mode (SMS) fiber structure (or single-mode–multimode fiber structure) has also been studied and developed to act as novel optical devices, e.g., a displacement sensor, a fiber lens, a refractometer sensor, an edge filter for wavelength measurements, and a bandpass filter [4]–[8]. These optical devices based on an SMS fiber structure offer all-fiber solutions for optical communications and optical sensing with the advantages of ease of packaging and connection to optical fiber system.

[4] and [5] investigated the single-mode–multimode fiber structure with an emphasis on the light propagation performance in the free-space after it comes out of the multimode fiber end. In [5], the guided-mode propagation analysis is used and an analytic expression of re-imaging distance was derived. [6] and [7] employed a numerical beam propagation method and through scanning the length of the multimode fiber section found a suitable value for desired applications. [8] demonstrated experimentally a bandpass filter based on the SMS fiber structure. In this paper, we present an investigation on the modeling of light propagation within the SMS fiber structure and an analysis of the multimode interference and the spectral response of the structure, which have not been addressed in the literature. There is another type of SMS fiber structure, of which the multimode fiber has a gradient index profile and no multimode interference occurs while the light propagates along the fiber structure [9]. In the present paper, the SMS fiber structure with a step-index multimode fiber is considered and the related multimode interference is investigated.

Section II investigates the modeling of light propagation within the SMS fiber structure. Based on the numerical calculation and experimental measurement, the reflection occurring at the interface between the single-mode fiber and multimode fiber (MMF) due to the mismatch of refractive index is found to be very small and can be neglected in practice. Therefore, a one-way guided-mode propagation analysis for the calculation of light propagation within the multimode fiber section and the calculation of coupling loss of the SMS fiber structure are presented. With an approximation to the eigenmode propagation constants of the MMF, the approximated guided-wave propagation analysis is derived and evaluated concerning the accuracy issue.

The characteristics of the multimode interference and the spectral response of the SMS structure are investigated in Section III. First, the phase conjugate characteristic of the light field about the half imaging distance $L_z/2$ is revealed. Second, a simple method is presented to predict the spectral response of the fiber structure without scanning the wavelength. With this simple method, it can be easily seen this SMS fiber structure can act as an edge filter at $L_z/4$ and $3L_z/4$ or a bandpass filter at L_z according to the relationship between the length of MMF and transmission. All these analysis and predictions are verified numerically and experimentally.

Conclusions are presented in Section IV.

II. Modeling of Light Propagation in the SMS Structure

A. modeling With the Guided-Mode Propagation Analysis

The single-mode–multimode–single-mode fiber structure is presented schematically in Fig. 1. The multimode fiber section has a step-index profile. The single-mode and multimode fibers are assumed to be aligned along the same axis, i.e., there is no offset between the single-mode and multimode fibers at the two interfaces.

There is usually a mismatch of the refractive index between the single-mode and multimode fibers, which can cause a reflection at the interface as shown in Fig. 1. To find out the re-

Manuscript received May 30, 2007; revised September 24, 2007. This work was supported by the Irish Research Council for Science, Engineering and Technology (IRCSET).

Q. Wang was with the Applied Optoelectronics Centre, School of Electronics and Communications Engineering, Dublin Institute of Technology, Dublin 8, Ireland. He is now with the Data Storage Institute, Singapore 117608, Singapore (e-mail: qian.wang@osa.org).

G. Farrell and W. Yan are with the Applied Optoelectronics Centre, School of Electronics and Communications Engineering, Dublin Institute of Technology, Dublin 8, Ireland (e-mail: Gerald.farrell@dit.ie).

Color versions of one or more of the figures in this paper are available online at http://ieeexplore.ieee.org.

Digital Object Identifier 10.1109/JLT.2007.915205

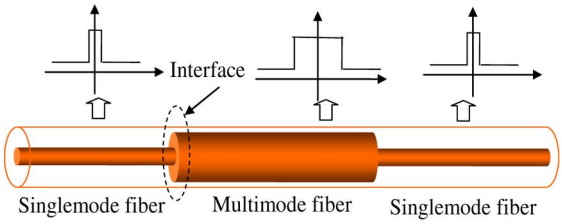

Fig. 1. Schematic configuration of the single-mode–multimode–single-mode fiber structure.

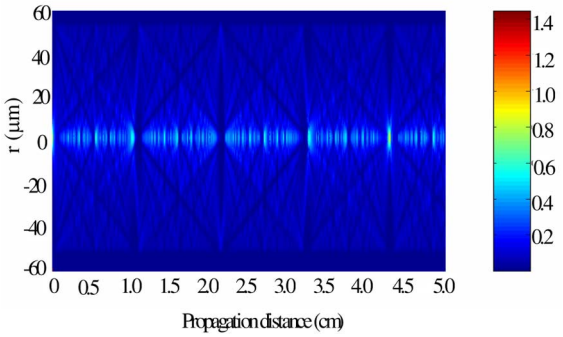

Fig. 2. Light propagation within the multimode fiber calculated by (3).

flectance at the interface, a beam propagation method in the time-domain for the circular symmetry waveguide developed in [10] or a simple Fresnel calculation can be employed and these two method lead to very close simulation results. As a numerical example, an SMF28 is chosen as the single-mode fiber section, of which the parameters are: the refractive index for the core and cladding is 1.4504 and 1.4447, respectively, at wavelength 1550 nm and the radius of core is 4.15 μm [11]. For practical refractive index of the multimode fiber core, which is around 1.5, the calculated reflectance with the above methods is very small ($< 0.2\%$).

For the experimental verification, the multimode fiber AFS105/125Y is chosen, of which the parameters are: refractive index for the core and cladding is 1.4446 and 1.4271, respectively. The core radius is 52.5 μm. The SMF28 is spliced with the MMF and the measured reflectance is around 50 dB through measuring the return loss of the structure. Therefore, the reflection occurring at the interface between the single-mode and multimode fibers is neglectable in practice and in the following modeling a one-way guided-mode propagation analysis is used to predict the light propagation within the fiber structure.

Due to the circular symmetric characteristic of fundamental mode of the single-mode fiber, the input light is assumed to have a field distribution of $E(r,0)$. When the light launches the multimode fiber, the input field can be decomposed by the eigenmodes $\{\mathrm{LP}_{nm}\}$ of the multimode fiber. Due to the circular symmetric of input field and an ideal alignment assumed above, only the LP_{0m} modes can be excited, which has been also addressed in [5]. Denote the field profile of LP_{0m} as $F_m(r)$, (the eigenmodes of the multimode fiber are normalized as $\int_0^\infty |E(r,0)|^2 r dr = \int_0^\infty |F_m(r)|^2 r dr$, $m = 1, 2, \ldots$) and

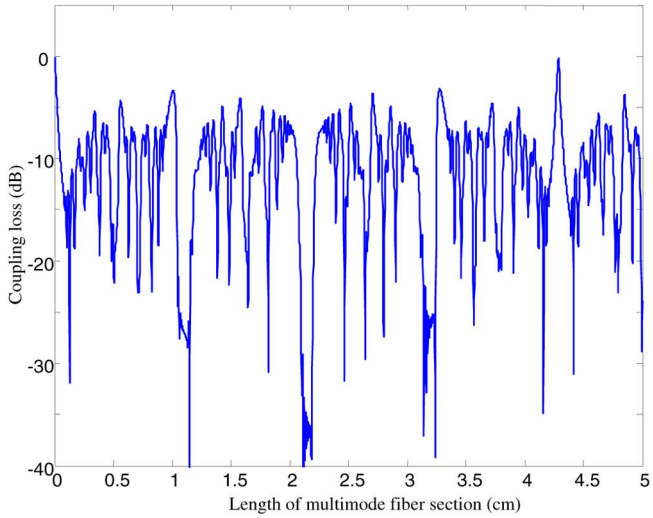

Fig. 3. Calculated coupling loss to output single-mode fiber for different MMF length.

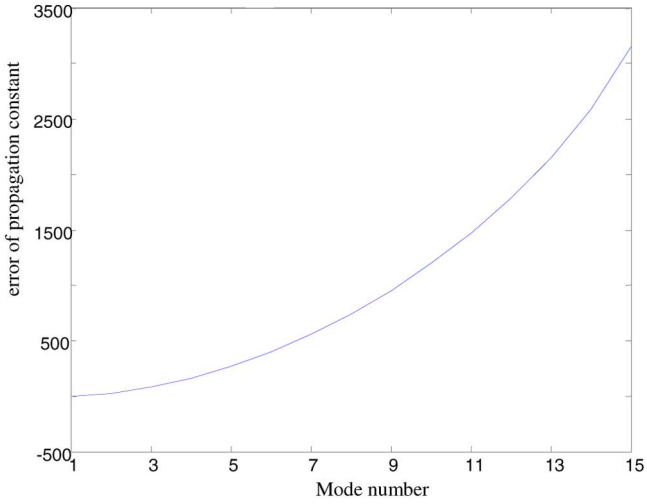

Fig. 4. Errors of approximated propagation constants.

neglect the small amount of radiation from the multimode fiber, we have

$$E(r,0) = \sum_{m=1}^{M} c_m F_m(r). \tag{1}$$

where c_m is the excitation coefficient of each mode and it can be calculated by the overlap integral between $E(r,0)$ and $F_m(r)$

$$c_m = \frac{\int_0^\infty E(r,0) F_m(r) r dr}{\int_0^\infty F_m(r) F_m(r) r dr}. \tag{2}$$

The excited mode number of the LP_{0m} multimode fiber $M \approx V/\pi$ ($V = \{2\pi/\lambda\} a \sqrt{n_{co}^2 - n_{cl}^2}$, where a is the radius of the multimode fiber core, n_{co} and n_{cl} is refractive index for the core and cladding of the multimode fiber, respectively and λ is the wavelength in the free-space).

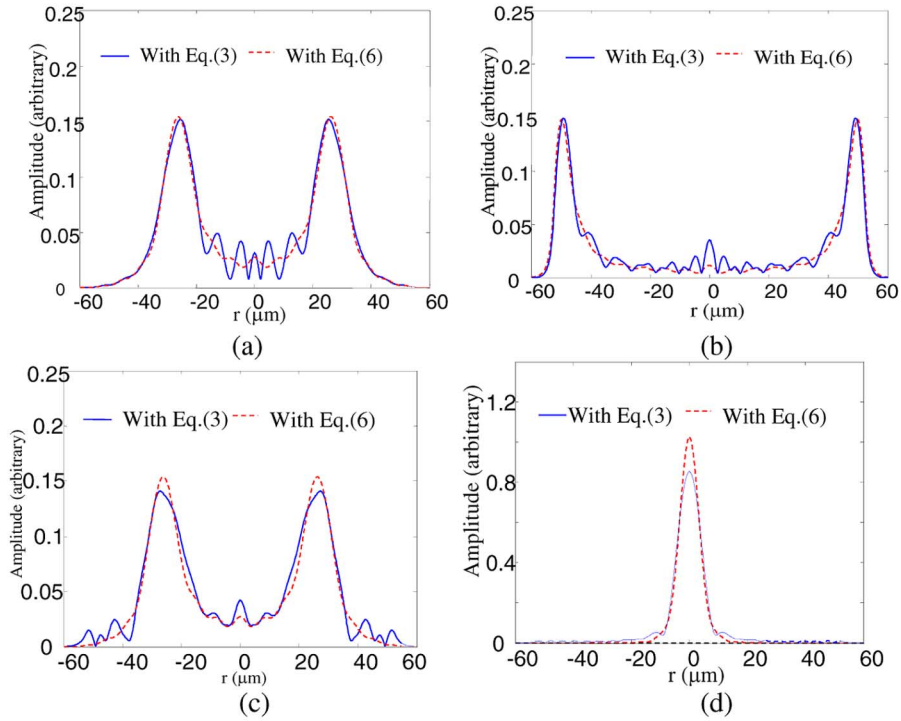

Fig. 5. Calculated lateral field profile with (3) and (6) at (a) $z = Lz/4$ and $\overline{L}_z/4$, (b)$z = Lz/2$ and $\overline{L}_z/2$, (c)$z = 3Lz/4$ and $3\overline{L}_z/4$, (d)$z = Lz$ and $\overline{L}_z$. Red curves are based on (6) and blue curves are based on (3).

As the light propagates in the multimode fiber section, the field at the propagation distance z can be calculated by [1], [5], [8]

$$E(r,z) = \sum_{m=1}^{M} c_m F_m(r) \exp(i\beta_m z). \tag{3}$$

where β_m is the propagation constant of each eigenmode of the multimode fiber.

As the numerical example, the multimode fiber AFS105/125Y is chosen and SMF28 is chosen as the input single-mode fiber. The considered light wavelength is 1550 nm in free-space. The multimode fiber has a step-index profile and so propagation constants can be calculated numerically with the well-known characteristic equation using the bisection method, which is easy for programming and has a good accuracy. Fig. 2 presents the amplitude of the calculated field along the multimode fiber. From Fig. 2 one can see the light spreads and converges while propagating along the multimode fiber, and it is re-imaged within the range $[4.0, 4.5]$ (cm) of the propagation distance.

As presented in Fig. 2, different propagation distances correspond to different field profiles at the cross-section. Therefore, coupling efficiency to the output single-mode fiber (i.e., the transmission of the SMS fiber structure) depends on the length of MMF. To calculate the transmission of the fiber structure, a conventional method is to employ the overlap integral between the light field $E(r,z)$ and eigenmode of the output single-mode fiber as shown in [5], In practice, the output single-mode fiber usually has the same fiber parameters with the input fiber, $f(r) = E(r,0)$. For this case, with the orthogonal relations between the eigenmodes of the MMF, the coupling loss can be calculated with the following [8]:

$$L_s(z) = 10\log_{10}\left(\left|\sum_{m=1}^{M} c_m^2 \exp(i\beta_m z)\right|^2\right). \tag{4}$$

For the above numerical example, the coupling loss is presented in Fig. 3. The exact re-imaging distance can be defined as the propagation distance with a maximal coupling efficiency. According to this definition, the re-imaging distance for this numerical example is $Lz = 42877\ \mu\text{m}$ with a coupling loss of -0.25 dB.

B. Approximated Guided-Mode Propagation Analysis-Formulation and Evaluation

The above equations provide a convenient modeling tool to predict the light propagation in the fiber structure and the transmission of the SMS fiber structure. However, in their current format they cannot offer a physical insight of the multimode interference occurring inside the multimode fiber section. To determine the light propagation characteristics in the multimode fiber section, an approximation to the propagation constants of the multimode fiber is taken.

For a step-index multimode fiber, it is known that the propagation constant of the mth mode can be approximated by [12]

$$\overline{\beta}_m \approx k_0 n_{co} - \left(2m - \frac{1}{2}\right)^2 \frac{\pi^2}{8k_0 n_{co} a^2} \tag{5}$$

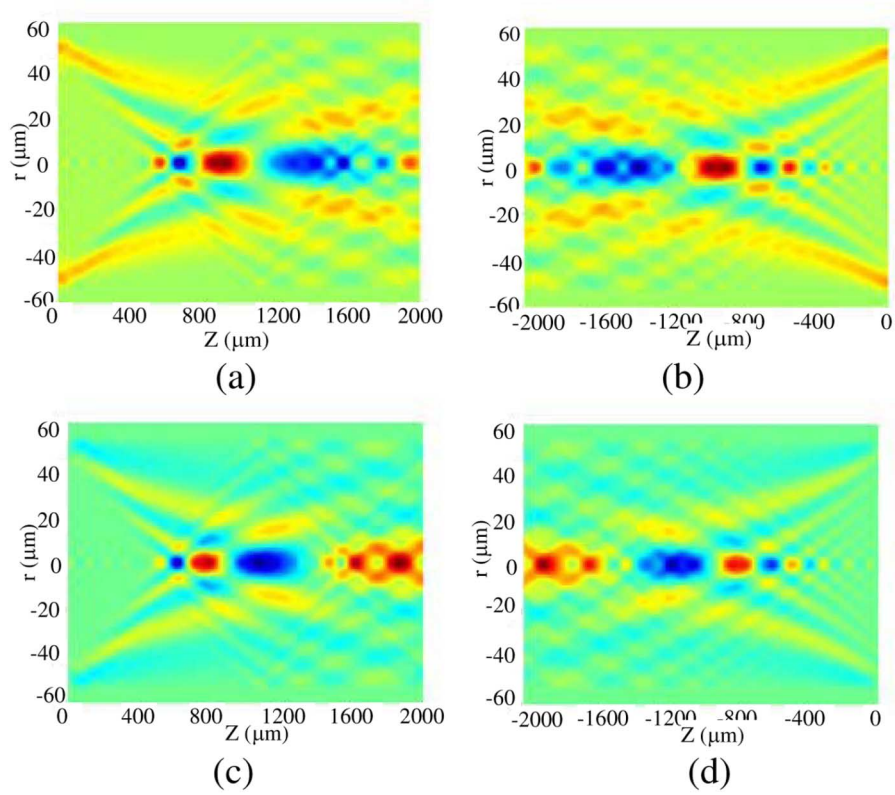

Fig. 6. Real part of calculated field for the: (a) first location range and (b) second location range. (c) Imaginary part of the calculated field for the first range. (d) Minus value of the imaginary part of the calculated field for the second range.

where $k_0 = 2\pi/\lambda$. Substituting this approximated propagation constant in (3) and it results in the following:

$$E(r,z) = \exp(\beta_1 z) \sum_{m=1}^{M} c_m F_m(r) \times \exp\left(-i\left(\frac{(2m+1)(2m-1)\pi}{\overline{L_z}}\right) z\right) \quad (6)$$

where $\overline{L}_z = 16 n_{co} a^2/\lambda$. In practical applications the common phase factor $(\exp(\beta_1 z))$ can be dropped. Correspondingly, with the approximation of propagation constants, the transmission of SMS fiber structure can be calculated by

$$L_s(z) = 10\log_{10} \times \left(\left|\sum_{m=1}^{M} c_m^2 \exp\left(-i\left(\frac{(2m+1)(2m-1)\pi}{\overline{L_z}}\right) z\right)\right|^2\right). \quad (7)$$

With (6) and (7), one can see when the propagation distance $z = \overline{L_z}$, the corresponding phase item $\exp(-i((2m+1)(2m-2)\pi)) = 1$ $(m = 1,2,\ldots)$. Therefore, $E(r,\overline{L_z}) = E(r,0)$ and $L_s(\overline{L}_z) = 0$ dB. This means that the light at $z = \overline{L_z}$ has the same lateral profile as the input, i.e., it is re-imaged at propagation distance $\overline{L}_z = 16 n_{co} a^2/\lambda$. It is identical to the result presented in [5], but the derivation procedure in the present paper is much simpler and intuitive as compared to that in [5], which involves the analysis of phase difference between excited eigenmode with the maximal excitation coefficient and other modes. The beat length between the first two eigenmodes is $L_\pi = 16 n_{co} a^2/10\lambda$ according to the approximated expression (5) of propagation constants. Thus, one can see the re-imaged distance $\overline{L}_z = 10 L_\pi$.

For the above numerical example, the approximated propagation constants $\overline{\beta}_m$ are calculated with (5) and the errors as compared to the real values β_m are shown in Fig. 4, from which it can be seen that the error increases for the high order eigenmodes and these errors cause the divergence between the approximated re-imaging distance and real value calculated with the formulation in Section II-A. With the approximations of the propagation constants, the re-imaging distance is $\overline{L}_s = 41101\ \mu$m. As compared to the re-imaging distance of $L_s = 42877\ \mu$m obtained in Section II-B, the relative error is -4.1%. For the propagation distance $\overline{L}_s = 41101\ \mu$m, the actual coupling loss is -15.3 dB. Therefore, in practical design of SMS fiber structure, the exact guided-mode propagation method should be used as the accuracy is concerned.

Our investigation indicates the above approximation only shortens the self-image distance of multimode interference from Lz to $\overline{L}_s$ but the simulations based on these two approaches have a similar multimode interference pattern. For the above numerical example, the lateral field profile calculated with (3) at a propagation distance of $Lz/4$, $Lz/2$, $3Lz/4$, and Lz is plotted in Fig. 5(a)–(d) with a blue curve, respectively. For comparison, the lateral field profile calculated with (6) at a propagation distance of $\overline{L}_z/4$, $\overline{L}_z/2$, $3\overline{L}_z/4$, and $\overline{L}_z$ is plotted in Fig. 5(a)–(d) with a red dashed curve, respectively. Obviously, the two calculation results are substantially similar.

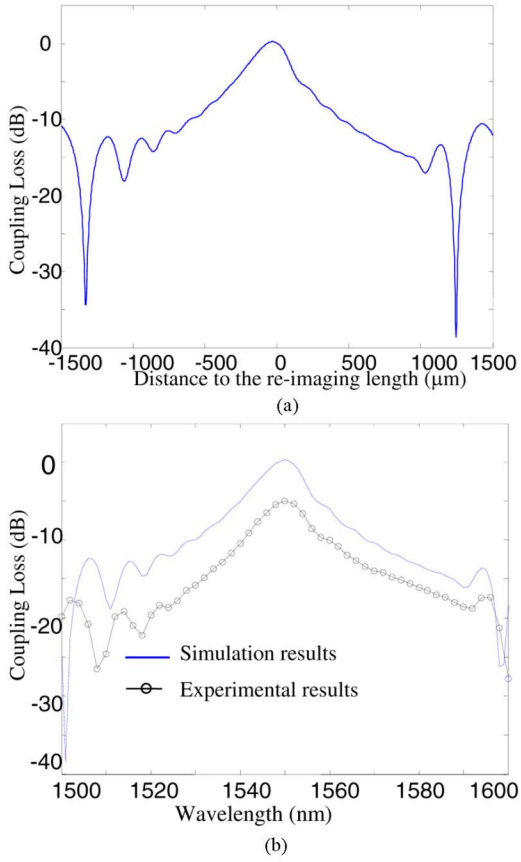

Fig. 7. (a) Coupling loss of the SMS fiber structure around the re-imaging distance. (b) Calculated and measured spectral response of the SMS fiber structure when the length of MMF fiber structure is L_z.

The approximated solution has less sidelobes as compared to the results obtained by the exact guided mode analysis, which is caused by the errors of propagation constant in the higher order modes. Although (6) and (7) are not recommended in practical design due to the accuracy issue, they are valuable in analyzing the multimode interference characteristics as shown below. In the below analysis, the approximated guided-mode propagation analysis is used for the analysis and prediction and the exact method is employed for the corresponding verification.

III. Characteristics of Multimode Interference and Spectral Response of the SMS Fiber Structure

A. Phase Conjugate of Light Field About $Lz/2$

For any propagation distance $z \in [0 \quad \overline{L}_z]$, the position can be represented by $z = \overline{L}_z/2(1+\delta)$ $(-1 \le \delta \le 1)$. According to the approximated (6) the corresponding light field is $E\left(r, \overline{L}_z/2(1+\delta)\right) = \sum_{m=1}^{M} c_m F_m(r)(-1)^{m-1} \exp[-i(2m+1)(m-1)\delta\pi]$. Then, the light field at the symmetric position of the plane $z = \overline{L}_z/2$, i.e., $z' = \overline{L}_z/2(1-\delta)$, has the form of $E(r, \overline{L}_z/2(1-\delta)) = \sum_{m=1}^{M} c_m F_m(r)(-1)^{m-1} \exp[i(2m+1)(m-1)\delta\pi]$. From these two expressions one can see that $E(r, \overline{L}_z/2(1+\delta)) = E^*(r, \overline{L}_z/2(1-\delta))$(symbol $*$ means conjugate). Therefore, the light fields at the position $z = \overline{L}_z/2(1+\delta)$ and $z' = \overline{L}_z/2(1-\delta)$ are phase conjugate about the plane $z = \overline{L}_z/2$.

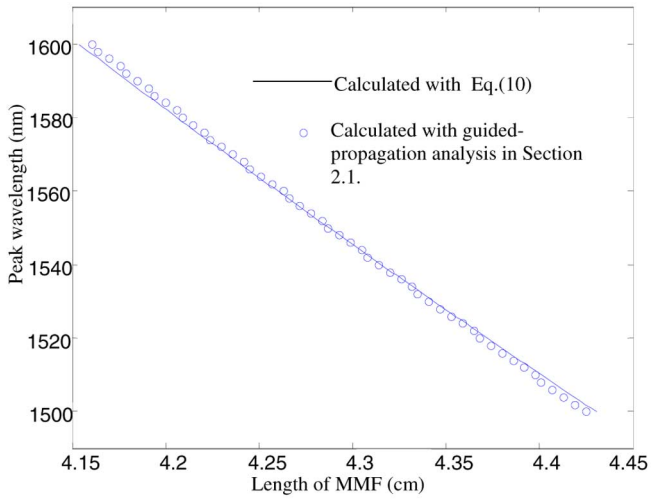

Fig. 8. Relationship between the peak wavelength and length of MMF.

To have a close look at this phase conjugate characteristic, the light field within the range of $[L_z/4 \quad L_z/4 + \Delta z]$ and the light field within the corresponding symmetric range of $[3L_z/4 - \Delta z \quad 3L_z/4]$ are compared as an example. The real parts of the calculated fields should be identical, i.e., $Re\{E(r, \overline{L}_z/2(1+\delta))\} = Re\{E(r, \overline{L}_z/2(1-\delta))\}$ and the imaginary part of the calculated fields should be opposite $Im\{E(r, \overline{L}_z/2(1+\delta))\} = Im\{E(r, \overline{L}_z/2(1-\delta))\}$. In the example, $\Delta z = 2000$ μm and the light field is calculated based on (3) (exact guided-mode propagation analysis). Fig. 6(a) and (b) presents the real part of calculated field for the two ranges respectively. Fig. 6(c) presents the imaginary part of the calculated field for the first range and Fig. 6(d) presents the minus value of the imaginary part of the calculated field for the second range. These two sets of identical patterns indicate the phase conjugate characteristic about $L_z/2$.

B. Wavelength Sensitivity of the SMS Structure

The coupling loss of the SMS fiber structure depends strongly on the length of the MMF as shown in Fig. 3, but it is also wavelength sensitive. The approximated (7) can be rewritten as below through substituting $\overline{L}_z = 16 n_{co} a^2/\lambda$

$$L_s(\lambda, z) = 10 \log_{10} \times \left(\left| \sum_{m=1}^{M} c_m^2 \exp(-i((2m+1)(2m-2)\pi) g(\lambda, z)) \right|^2 \right) \quad (8)$$

where $g(\lambda, z) = \lambda z/16 n_{co} a^2$. Neglecting the wavelength dependence of the excitation coefficient c_m and the material dispersion of the fiber core n_{co} (the numerical examples below indicate that this is reasonable), we can see that the transmission of the fiber structure with a wavelength shift equals to that with a length variation of MMF, i.e., $L_s(\lambda_0 + \Delta\lambda, z_0) = L_s(\lambda_0, z_0 + \Delta z)$, only if

$$\frac{\Delta\lambda}{\lambda_0} = \frac{\Delta z}{z_0}. \quad (9)$$

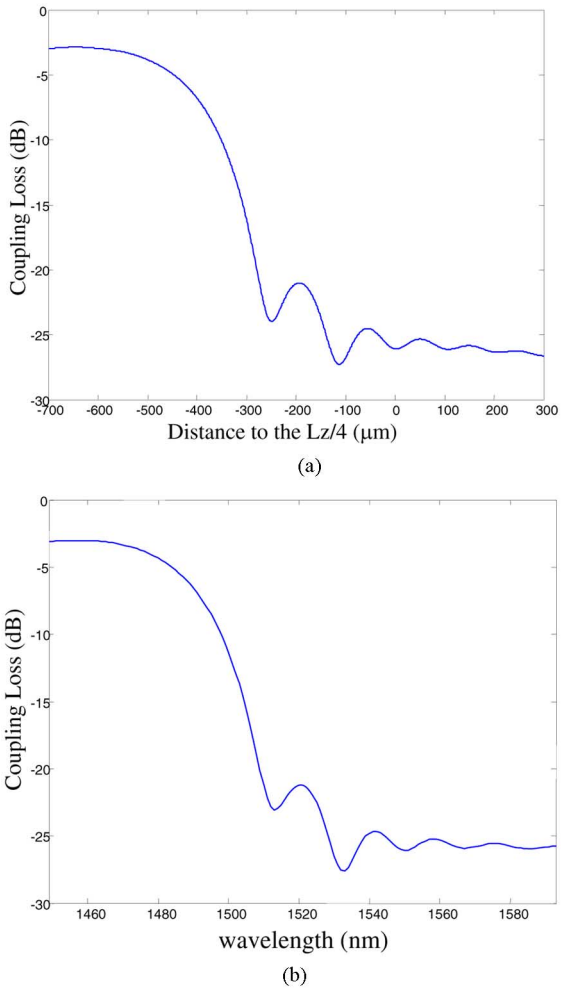

Fig. 9. (a) Coupling loss of the SMS fiber structure around $L_z/4$ and (b) spectral response of the SMS fiber structure when the length of MMF fiber structure is $L_z/4$.

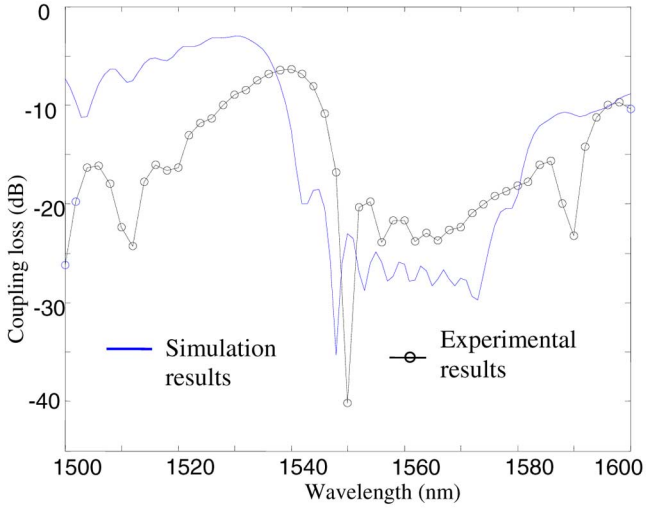

Fig. 10. Calculated and measured spectral response of the SMS fiber structure when the length of MMF fiber structure is $5L_z/4$.

Therefore, the wavelength dependence of the structure can be easily predicted based on coupling loss under different length of the MMF as shown in Fig. 3, instead of the wavelength scanning as in [7]. From Fig. 3 we can see that the SMS fiber structure can act as an bandpass filter when the length of MMF is L_z and it is an edge filter when the length of MMF around $L_z/4$ and $3L_z/4$, respectively. To verify these predictions, numerical simulations and experimental verifications are presented as follows.

1) **Bandpass filter at the re-imaging distance**: for wavelength 1550 nm, the coupling loss of the SMS fiber structure around the re-imaging distance $L_z = 42877\ \mu\text{m}$ is shown in Fig. 7(a). According to (9), with $\Delta z = 1500\ \mu\text{m}$, the structure has the same spectral response within $\Delta\lambda = 54$ nm, i.e., $[1496, 1604]$ (nm). As a verification, the coupling loss of the SMS fiber structure within the wavelength rang $[1500, 1600]$ (nm) is calculated with (4) and measured experimentally. The corresponding results are presented in Fig. 7(b). One can see that both the numerical and experimental results are close to the coupling loss presented in Fig. 7(a).

For a given length of MMF, the peak wavelength of the bandpass filter can be found by simulating light propagation using the guided-mode propagation analysis presented in Section II-A. Alternatively, it can also be determined based on (8) with a good accuracy. For the SMS fiber structure with a length L_0 of the MMF, the corresponding peak wavelength of the bandpass filter is assumed to be λ_0. When the length of multimode fiber is change to be $L_1 = L_0 + \Delta L$, the shift of peak wavelength $\Delta\lambda$ can be calculated approximately according to (8), i.e., $L_s(\lambda_0, L_0) = L_s(\lambda_0 + \Delta\lambda, L_0 + \Delta L)$, which leads to

$$\Delta\lambda = -\frac{\Delta L}{L_0}\lambda_0. \tag{10}$$

Fig. 8 gives the relationship between the peak wavelength and length of MMF for the above numerical example with (10) and guided-propagation analysis respectively, from which it can be seen that they are in good agreement.

2) **Edge filter (from high to low)**: coupling loss of the SMS fiber structure around $L_z/4$ with a considered length range of the MMF fiber from $Lz/4 - 700\ \mu\text{m}$ to $Lz/4 + 300\ \mu\text{m}$ at a wavelength 1550 nm is presented in Fig. 9(a). With (9), the corresponding wavelength range is from 1449 to 1593 nm, and within this wavelength range the fiber structure has a same transmission as presented in Fig. 9(a). Corresponding verification with (4) is presented in Fig. 9(b), from which one can see it is an edge filter with a transmission from high to low and it can be employed in wavelength measurements within the wavelength range with monotonic decreasing coupling loss as proposed in [7], of which the design is scanning the MMF length based on a BPM simulation.

Due to the assembling difficulty when the length of MMF is $L_z/4$ (it is less than 1 cm in the experiment), a length of $5L_z/4$ is chosen instead. For the length of $5L_z/4$,

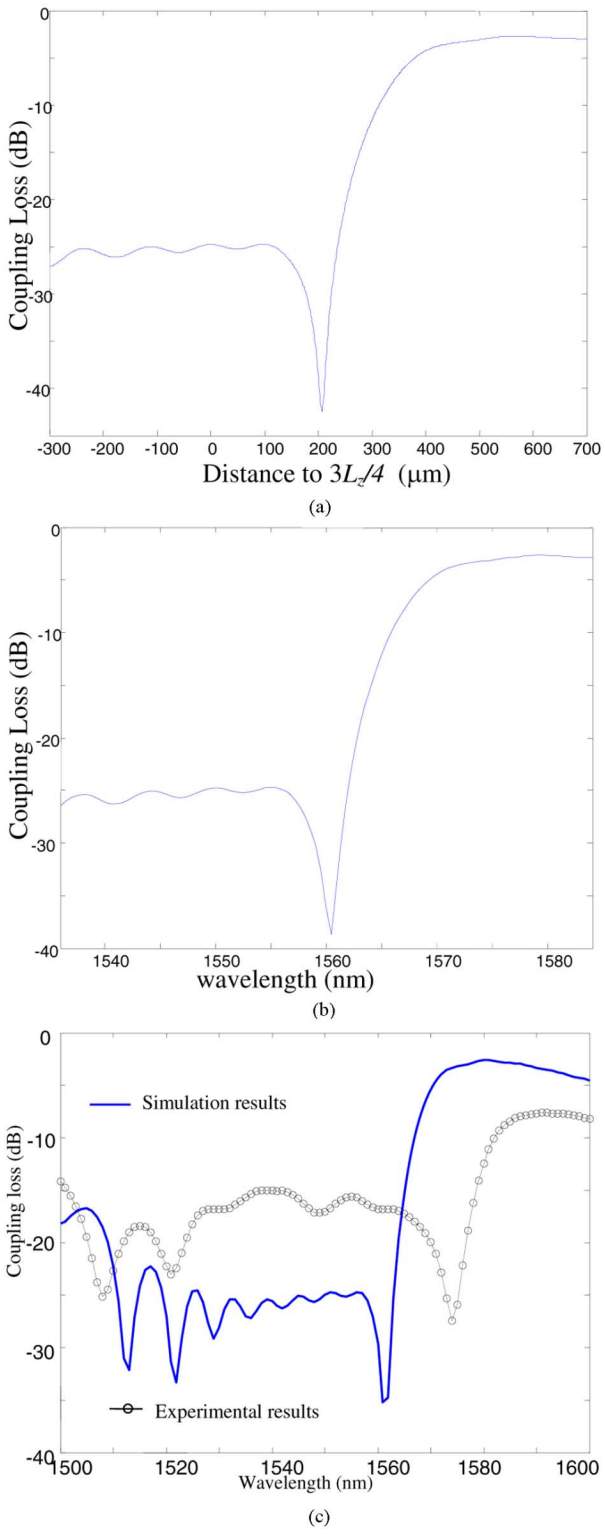

Fig. 11. (a) Transmission loss of the SMS fiber structure around $3Lz/4$ and (b) spectral response of the SMS fiber structure when the length of MMF fiber structure is $3Lz/4$.

the SMS fiber structure also behaves as an edge filter from high to low as shown in Fig. 10.

3) **Edge filter (from low to high)**: transmission of the SMS fiber structure around $3L_z/4$ with a considered length range of the MMF fiber from $3Lz/4 - 300$ μm to $3Lz/4 + 700$ μm is presented in Fig. 11(a). With (9), within the wavelength range from 1535.5 to 1583.7 nm, the fiber structure with a MMF length of $Lz/4$ has a same transmission as presented in Fig. 11(a). Corresponding verification with (4) is presented in Fig. 11(b), from which one can see it is also an edge filter. But as compared to the above case, it has a steeper transition and the transmission is from low to high with wavelength. The experimental verification of edge filter at $3L_z/4$ is presented in Fig. 11(c), which also shows a transition of transmission from low to high.

IV. Conclusion

The single-mode–multimode–single-mode fiber structure with a step-index profile has been investigated theoretically and experimentally in this paper. The reflection at the interface between the single-mode and multimode due to the mismatch of fiber refractive index is found to be very small and can be neglectable in practice. Therefore, a one-way guided-mode propagation analysis for the circular symmetry waveguide has been employed to model the light propagation and with an approximation to the propagation constants of the eigenmodes for the multimode fiber, the approximated formulations have been derived and evaluated. The evaluation example indicates that this approximated guided-mode propagation method is not recommended for practical design due to the accuracy issue, but it is useful in analysis and prediction of the device performance. With the derived approximated formulation, the phase conjugate of the light field about $L_z/2$ has been discussed and verified with the exact modeling method. Finally, a simple method to predict the wavelength sensitivity of the SMS fiber structure is developed, from which it can be seen that the SMS fiber structure can act as a band pass filter or edge filter depending on the length of MMF. The prediction using the simple method has been verified numerically and experimentally.

References

[1] L. B. Soldano and E. C. M. Pennings, "Optical multi-mode interference devices based on self-imaging: Principles and applications," *J. Lightwave Technol.*, vol. 13, pp. 615–627, 1995.

[2] B. M. A. Rahman, N. Somasiri, C. Themistos, and K. T. V. Grattan, "Design of optical polarization splitters in a single-section deeply etched MMI waveguide," *Appl. Phys.*, vol. B 73, pp. 613–618, 2001.

[3] M. R. Paiam and R. I. MacDonald, "Design of phased-array wavelength division multiplexers using multimode interference couplers," *Appl. Opt.*, vol. 36, no. 21, pp. 5097–5108, 1997.

[4] A. Mehta, W. S. Mohammed, and E. G. Johnson, "Multimode interference-based fibre optic displacement sensor," *IEEE Photon. Technol. Lett.*, vol. 15, pp. 1129–1131, 2003.

[5] W. S. Mohammed, A. Mehta, and E. G. Johnson, "Wavelength tunable fibre lens based on multimode interference," *J. Lightwave Technol.*, vol. 22, pp. 469–477, 2004.

[6] Q. Wang and G. Farrell, "All-fibre multimode-interference based refractometer sensor: Proposal and design," *Opt. Lett.*, vol. 31, no. 3, pp. 317–319, 2006.

[7] Q. Wang and G. Farrell, "Multimode fibre based edge filter for optical wavelength measurement application," *Microw. Opt. Technol. Lett.*, vol. 48, no. 5, pp. 900–902, 2006.

[8] W. S. Mohammed, P. W. E. Smith, and X. Gu, "All-fibre multimode interference bandpass filter," *Opt. Lett.*, vol. 31, no. 17, pp. 2547–2549, 2006.

[9] D. Donlagic and M. Zavrsnik, "Fibre-optic microbend sensor structure," *Opt. Lett.*, vol. 22, no. 11, pp. 837–839, 1997.
[10] J. Shibayama, T. Takahashi, J. Yamauchi, and H. Nakano, "Efficient time-domain finite-difference beam propagation methods for the analysis of slab and circularly symmetric waveguides," *J. Lightwave Technol.*, vol. 18, pp. 437–442, 2000.
[11] Q. Wang, G. Farrell, and T. Freir, "Theoretical and experimental investigations of macro-bend losses for standard single mode fibres," *Opt. Express*, vol. 13, no. 12, pp. 4476–4484, 2005.

Qian Wang received the Ph.D. degree in optical engineering from Zhejiang University, Hangzhou, China, in 2004.

He worked as a Visiting Research Scientist in Alfven Laboratory, Royal Institute of Technology, Sweden, in 2003 and a Senior Researcher in the Applied Optoelectronics Centre, Dublin Institute of Technology, Dublin, Ireland, in 2004. In 2007, he joined the Data Storage Institute, under the agency for Science, Technology and Research, Singapore, as a Senior Research Fellow. He is interested in modeling and simulation, design and optimization of micro-photonic and nano-photonic components and developing their applications in communication, sensing, imaging, etc. He has published over 60 papers in academic journals in these areas to date.

Gerald Farrell graduated with an honours degree in electronic engineering from University College Dublin, Dublin, Ireland, in 1979 and the Ph.D. degree from Trinity College, Dublin, in 1993.

He spent a number of years as a Design Engineer in the Transmission Division of Telectron Ltd. Between 1989 and 1993, he carried out research in optical synchronization using self-pulsating laser diodes at Trinity College, leading to a Ph.D. degree and resulting in the development and patenting of a new method of all-optical frequency changing. Since 2000, he has been Director of the Applied Optoelectronics Centre at the Dublin Institute of Technology. He has been a consultant to a variety of organizations in Ireland and abroad. Areas of expertise include optical fibre systems, RF and analogue circuit design and communications systems planning. He has both delivered and organized a variety of training courses in optical communications and has published a significant number of papers in the areas of optical communications and laser diode applications.

Wei Yan, photograph and biography not available at the time of publication.